

# Probiotic Pre-Treatment Protects Kidneys Exposed to Microcystin-LR

Yolanda Hu<sup>a\*</sup>, Irene Sun<sup>a\*</sup>, Eric Tang<sup>a\*</sup>, William Ryan<sup>‡b</sup>, Upasana Shreshtha<sup>3c</sup>, Jyotshana Gautam<sup>3c</sup>, Apurva Lad<sup>3c</sup>, Jason F. Huntley<sup>2d</sup>, Steven Haller<sup>3c</sup>, David Kennedy<sup>3c</sup>

<sup>a</sup> Summer Biomedical Science Program in Bioinformatics, Department of Neurosciences, Toledo, Ohio. (3000 Arlington Avenue, Mail Stop 1007, Health Science Campus, The University of Toledo, Toledo, Ohio 43615) 419.383.4210

<sup>b</sup> Department of Neurosciences, Toledo, Ohio. (3000 Arlington Avenue, Mail Stop 1007, Health Science Campus, The University of Toledo, Toledo, Ohio 43615) 419.383.4210

<sup>c</sup> Department of Medicine, Toledo, Ohio. (3000 Arlington Avenue, Mail Stop 1007, Health Science Campus, The University of Toledo, Toledo, Ohio 43615) 419.383.4210

<sup>d</sup> Department of Medical Microbiology and Immunology, Toledo, Ohio. (3000 Arlington Avenue, Mail Stop 1007, Health Science Campus, The University of Toledo, Toledo, Ohio 43615) 419.383.4210

\* equal contribution

‡ corresponding author

E-mail: William.Ryan2@rockets.utoledo.edu

Published Date: 18 January 2024

## Abstract

Cyanobacterial Harmful Algal Blooms (CyanoHABs) occur when colonies of photosynthetic bacteria called cyanobacteria grow out of control, usually in warm, nutrient-rich, slow-moving waters. They are becoming increasingly prevalent around the world and release harmful toxins called cyanotoxins into bodies of water, which negatively affect human and ecological health. One such cyanotoxin is microcystin, with microcystin-leucine arginine (MC-LR) being the most widespread. Exposure to MC-LR inhibits serine and threonine protein phosphatase 1 and 2A in humans, causing a myriad of health problems. Fortunately, naturally occurring bacteria may be able to degrade MC-LR and reverse its effects. Mice were separated into five experimental groups based on three types of pre-treatments (control drinking water/vehicle, probiotic-supplemented drinking water, and heat-inactivated probiotic-supplemented drinking water) as well as two types of exposures (microcystin-LR and water/vehicle). RNA was extracted from kidneys for sequencing because MC-LR exacerbates kidney disease. Gene expression data were analyzed with 3 Pod Reports, an R software package for comprehensive transcriptomic pathway analyses. MC-LR exposure was associated with upregulated cellular respiration and metabolism pathways and downregulated transcription pathways. Probiotic pre-treatment combined with MC-LR exposure was associated with upregulated lipoprotein particle pathways and downregulated respiration and ribosome pathways. Overall, the probiotic mixture reversed the transcriptional profile resulting from MC-LR exposure. Future high-yield pathways that could be targeted for therapeutic benefit include VEGFR inhibitors and increased expression of renal indicator genes such as EGFR.

Keywords: harmful algal blooms, cyanobacteria, mice, microcystin, kidneys, probiotic

## 1. Introduction

There are many varieties of algae, including brown diatoms and green algae. However, most Harmful Algal Blooms (HABs) are chiefly composed of photosynthetic bacteria called cyanobacteria, also known as blue-green algae (1, 2). These Cyanobacterial Harmful Algal Blooms (CyanoHABs) occur when cyanobacteria grow out of control in nutrient-rich, warm, and slow-moving waters, which are becoming increasingly common across the world (1, 3). Major causes of CyanoHABs include climate change and increased eutrophication of water bodies that provide abundant resources promoting the proliferation of cyanobacteria (3). In fact, more than 40% of lakes and reservoirs in Europe, Asia, and America possess conditions for CyanoHABs, with 25–75% of resulting blooms being considered toxic (2).

### 1.1 MC-LR

Some cyanobacteria release toxic chemicals called cyanotoxins, such as microcystin (MC), into the water, which have severe consequences for human health at all levels (1). One cyanotoxin is microcystin, a cyclic heptapeptide consisting of seven amino acids, two of which are variable and determine the specific class of microcystin (4). While there are over 200 congeners of microcystin, one of the most widespread is microcystin-leucine arginine (MC-LR) (1).

### 1.2 How does MC-LR cause damage?

There are multiple routes of exposure to MC-LR, mainly ingestion of contaminated food, water, or supplements, inhalation of CyanoHAB toxins as aerosols in the air, and dermal contact through activities such as swimming in contaminated waters (5). Once MC-LR has entered the human body, it inhibits serine and threonine protein phosphatase 1 and 2A (1, 6). This leads to hyperphosphorylation, which disrupts cells and alters the cytoskeleton with major disruption of cells, such as cell lysis (1, 7). Additionally, since phosphatases serve vital regulatory functions of cell signaling related to critical processes, their inactivation by MC-LR has potent and far-reaching effects. This can lead to downstream consequences including the promotion of oxidative stress, inflammation, apoptosis, and carcinogenic effects (1, 8).

### 1.2 What does MC-LR damage?

Although microcystins are classified as hepatotoxin, they cause effects throughout the body, including in other vital organs such as the lungs and kidneys (1). The effects of microcystin on the kidneys may be of particular importance due to their contribution to the metabolism of xenobiotics such as MC-LR. MC-LR and its metabolites, MC-LR-glutathione

and MC-LR-cysteine, accumulate in the kidneys which can exacerbate chronic kidney disease, leading to kidney failure (9). Recently, with the increase in HABs, there has been increased exposure to harmful microcystins. Most notably, one such event occurred in Brazil in 1996, when 116 of 130 (89%) patients receiving renal dialysis treatment developed headaches, eye pain, blurred vision, and nausea as a direct result of exposure to cyanobacterial hepatotoxins (10). Shortly after, 100 of these patients with end-stage renal disease developed acute liver failure, and over half died (10).

Because of the tremendous health effects of these toxins, several attempts have been made to develop treatments and discover therapies. Fortunately, recent research has shown that certain naturally occurring bacteria, including strains of *Lactobacillus* and *Bifidobacteria*, have demonstrated an ability to degrade MC-LR into a linear form and reverse its effects both *in vitro* and *in vivo* (11, 12). They reverse the effects of MC-LR by inducing the recovery of antioxidative levels to reach a balance with reactive oxygen species, effectively reducing oxidative stress generated by MC-LR. To remove MC-LR, past studies have suggested that bacteria degrade it, which makes it non-toxic (13). Thus, we tested the hypothesis that bacteria with the capacity to break down MC-LR may reduce its effects. We tested this hypothesis by pre-treating mice with a probiotic mixture and then assessed the impact of MC-LR on transcript expression in the renal parenchyma.

## 2. Methods

### 2.1. Mice Treatment and Exposure

All procedures were approved by the University of Toledo IACUC on 02/09/2016 and performed in accordance with the US Animal Welfare Act (Office of Animal Welfare Number 10-8663). BALB/c mice were separated into five experimental groups and comparisons based on three types of pre-treatments (control drinking water/vehicle, probiotic-supplemented drinking water, and heat-inactivated probiotic-supplemented water) as well as two types of exposures (microcystin-LR and water/vehicle). Each group represented  $n = 3$  biologically distinct replicates with no technical replicates. All pre-treatments were administered *ad libitum* for the duration of four weeks by preparing an equal volume of all bacteria each adjusted to OD<sup>600</sup> of 0.5. The MC-LR degrading bacteria present in the live-probiotic solution consisted of an average mixture of *Cellulophaga sp.* ( $8.3 \times 10^3$  CFU/mL), *Sphingobium yanoikuyae* ( $4.7 \times 10^3$  CFU/mL), *Rhizobium sp.* ( $1 \times 10^5$  CFU/mL), *Porphyrobacter sp.* ( $7.2 \times 10^3$  CFU/mL), and *Pseudomonas sp.* ( $1.3 \times 10^4$  CFU/mL) as previously isolated and purified for a total of  $1.4 \times 10^5$  CFU/mL. The MC-LR degrading bacteria present in the heat-inactivated

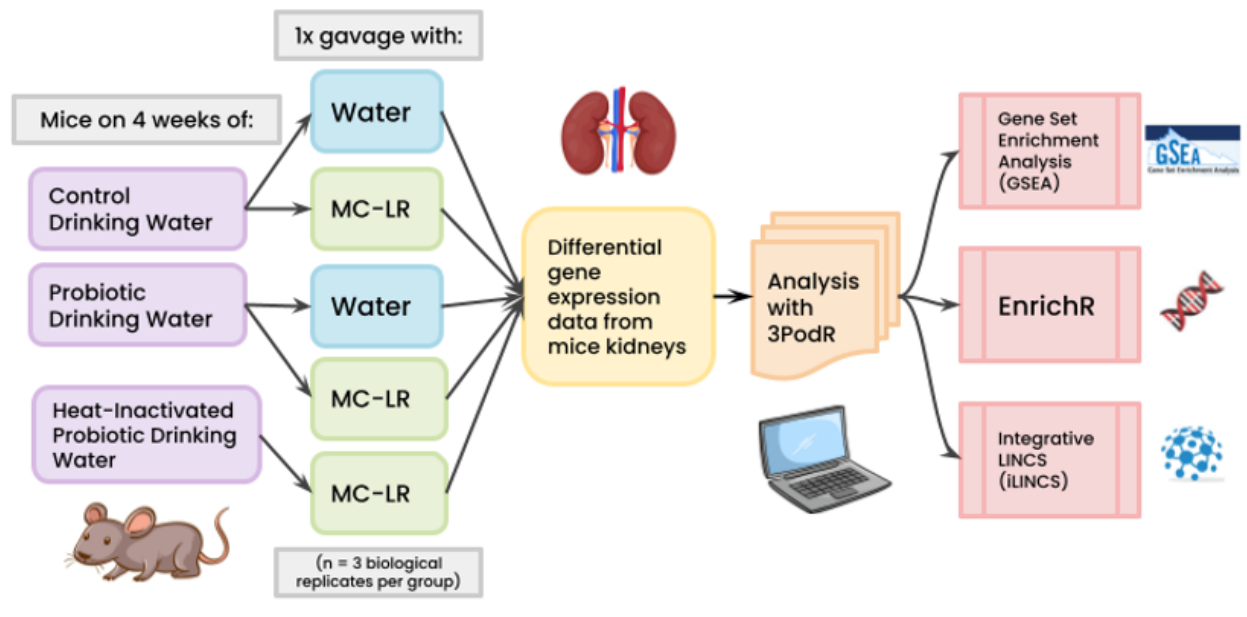


**Figure 1.** Workflow of study. Mice ( $n = 3$  biological replicates per group) were separated into groups and administered the pre-treatment of control drinking water/vehicle, probiotic-supplemented drinking water, or heat-inactivated probiotic drinking water for four weeks. Next, mice were exposed to a one-time challenge of either microcystin-LR or water via gavage. After 24 hours, harvested kidneys were frozen and split in preparation for RNA extraction. Differential Gene Expression data for each group was analyzed and compared using GSEA, EnrichR, and iLINCS.

probiotic solution consisted of a mixture of *Cellulophaga sp.* ( $2.6 \times 10^2$  CFU/mL), *Sphingobium yanoikuyae* ( $7.6 \times 10^3$  CFU/mL), *Rhizobium sp.* ( $7.4 \times 10^4$  CFU/mL), *Porphyrobacter sp.* ( $1.7 \times 10^4$  CFU/mL), and *Pseudomonas sp.* ( $2.5 \times 10^4$  CFU/mL) as previously isolated and purified for a total of  $1.2 \times 10^5$  CFU/mL. After four weeks, the mice were exposed to a one-time challenge of MC-LR (500 ug/Kg) or vehicle (water) via a gavage. Twenty-four hours after the challenge, the mice were euthanized, and their kidneys were snap-frozen at  $-85^\circ\text{C}$  and prepared for RNA extraction (Figure 1).

RNA was extracted using the RNeasy Plus Mini Kit (Cat # 74136, Qiagen) as previously described (14-16). A sequencing library for Poly (A) sequencing was prepared according to Illumina's mRNA sample preparation, followed by paired-ended sequencing (14-16). According to FastQC generated quality control information, low-quality, unknown, and contaminated bases/reads were removed. HISAT2 with featureCounts was used to align and count reads to the mouse genome (GRCm38).

Although there were five total comparisons, we focused on three: MC-LR vs. Vehicle, MC-LR + Probiotic vs. MC-LR + Heat-Inactivated Probiotic, and MC-LR + Probiotic vs. MC-LR. The first group, MC-LR vs. Vehicle, compared mice given control drinking water then exposed to MC-LR and mice given control drinking water then exposed to water. This comparison was necessary to discern the effects of MC-LR on the kidneys without any pre-treatment. The next group, MC-LR + Probiotic vs. MC-LR + Heat-Inactivated Probiotic compared the gene expression of mice given probiotic-

supplemented drinking water then exposed to MC-LR and mice given heat-inactivated probiotic-supplemented drinking water then exposed to MC-LR. This was essential to ensure any differences between the control drinking water group and the probiotic drinking water group when exposed to the MC-LR challenge were caused by the activity of the live bacteria and not simply its presence. Finally, MC-LR + Probiotic vs. MC-LR contrasted the effects of MC-LR on mice given probiotic-supplemented drinking water then exposed to MC-LR and mice given control drinking water then exposed to MC-LR. This comparison was imperative to observe the ability of the bacterial probiotic mixture to reverse the effects of MC-LR. The order of MC-LR + Probiotic vs. MC-LR + Heat-Inactivated Probiotic and MC-LR + Probiotic vs. MC-LR comparisons is healthier vs. exposed, so we expect that the differentially expressed genes (DEGs) of MC-LR vs. Vehicle to be inverses of the other two comparisons as it is exposed (MC-LR with no pre-treatment) vs. healthier (no exposure to MC-LR).

## 2.2. Datasets and 3 Pod Reports

Our final processed dataset consisted of the  $\log_2$  fold-change, p-value, p-adjusted value, gene names, and sample IDs stored in a .csv file as provided by Azenta Life Sciences, which was then processed using a bespoke R package, 3 Pod Reports. 3 Pod Reports takes differential gene expression

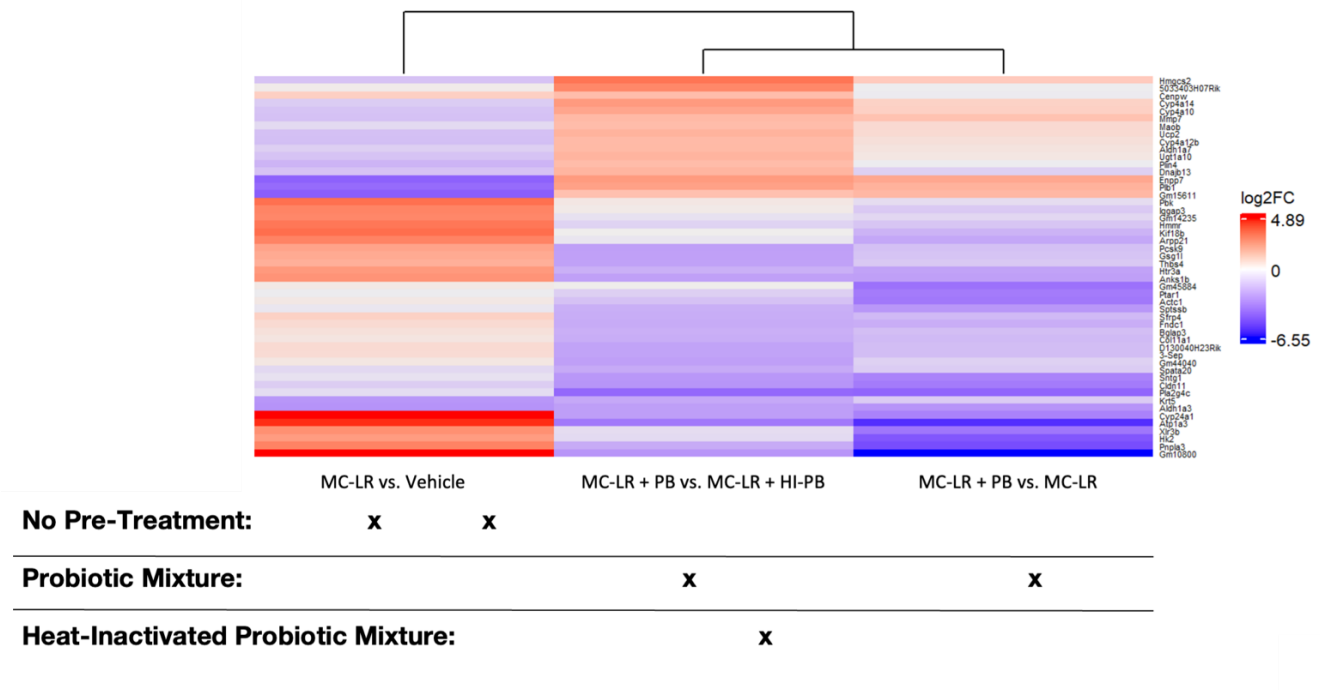


**Figure 2.** Heatmap comparing the differential gene expression of the three comparisons. MC-LR + Probiotic vs. MC-LR + Heat-inactivated Probiotic and MC-LR + Probiotic vs. MC-LR are very similar regarding upregulated and downregulated genes, while MC-LR vs. Vehicle appears to be the inverse of the two. Red means upregulated and blue means downregulated, with the saturation of color corresponding to the log<sub>2</sub> fold-change. The Xs below each group indicate which pre-treatment they received. Abbreviations: PB, probiotic; HI-PB, heat-inactivated probiotic; MC-LR, Microcystin-leucine-arginine.

data and yields a report consisting of Gene Set Enrichment Analysis (GSEA), EnrichR, and integrative LINCS (iLINCS) (17).

### 2.3. Pathway Analysis

Gene Set Enrichment Analysis (GSEA) was used to perform full transcriptome analyses. The top upregulated and downregulated pathways were determined using GSEA from an input of ranked genes by p-value and log<sub>2</sub> FC, while (log<sub>2</sub>FC) \* (-log<sub>10</sub>(PValue)) was used as a ranking metric. The *fgsea* R package (version 1.16.0) was used to run GSEA quickly and accurately. GSEA uses the full list of ranked genes instead of individual genes, and top pathways are determined by p-value and enrichment scores (18). The Gene Ontology pathway package was used to define the gene sets (18, 19).

The enrichR R package was used to perform gene-set overrepresentation analysis with the top 10% up and downregulated differentially expressed genes (p<0.05) by

log<sub>2</sub>FC (20). EnrichR was used to generate combined scores to identify pathways that are significantly up or downregulated from a given list of DEGs (20).

These two methods provide complementary strengths for a more comprehensive analysis. GSEA better reflects small, subtle changes in gene expression, while EnrichR identifies the top changes (18, 20).

### 2.4. Leading Edge Gene Analysis

In addition to pathway analysis, GSEA also provides a leading edge (LE) gene analysis in which the genes that are most influential for the up or downregulation of significant pathways are identified. LE genes are a core subset of genes that contribute significantly to the enrichment score of pathways. To determine the LE genes of a pathway, three statistics are used: Tags, List, and Signal. Tags determine the percentage of genes from a set that contribute to a pathway's enrichment score. List ascertains the genes that are before (positive) or after (negative) the apex of a pathway's

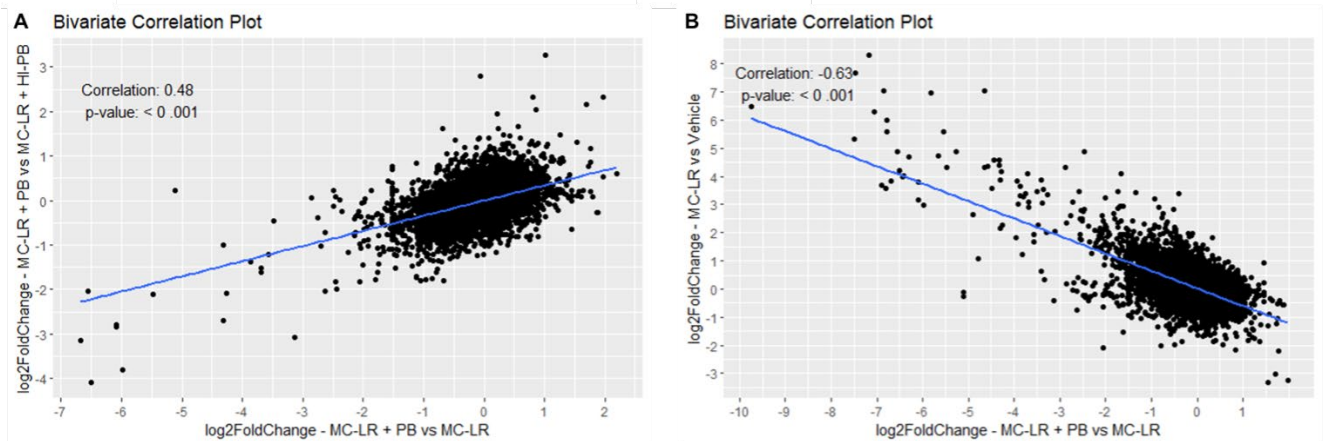


**Figure 3.** (a) Bivariate plot illustrating the correlation between the differential gene expression of MC-LR + Probiotic vs. MC-LR + Heat-inactivated Probiotic and MC-LR + Probiotic vs. MC-LR alone ( $n = 16507$ ,  $r = 0.48$ ;  $P < .001$ ). There is a significant and moderately strong positive correlation between the differential gene expressions indicating similarity between MC-LR and MC-LR Heat-inactivated Probiotic. (b) Bivariate plot illustrating the correlation between the differential gene expression of MC-LR vs. Vehicle and MC-LR + Probiotic vs. MC-LR ( $n = 16880$ ,  $r = -0.63$ ,  $P < 0.001$ ). There is a significant and strong negative correlation between the differential gene expression of MC-LR vs. Vehicle and MC-LR + Probiotic vs. MC-LR, indicating that probiotic is reducing the effect of MC-LR on gene expression so that its expression is like that of vehicle. If the order of the comparison MC-LR vs. MC-LR + Probiotic was flipped, then MC-LR + Probiotic would be in the same position as Vehicle compared to MC-LR. The blue line is generated from a linear model. Abbreviations: PB, probiotic; HI-PB, heat-inactivated probiotic; MC-LR, Microcystin-leucine-arginine.

enrichment score from a ranked gene list. Finally, signal combines the statistics of Tags and List to identify leading edge genes (18). Leading edge genes can be used to determine which genes are “driving” the majority of the observed enrichment. We focused specifically on analyzing the genes that overlap between multiple leading-edge subsets.

### 2.5. iLINCS Perturbagen Identification

The Library of Integrated Network-based Cellular Signatures (LINCS) is an initiative by the National Institute of Health aiming to create a network of molecular responses to both environmental and internal stressors. This project uses the L1000 assay, a gene expression array of 978 landmark genes, to generate gene signatures that predict the expression of over 11,000 more genes (21). In the dataset, the  $\log_2$  fold-change and p-value for genes in the LINCS L1000 project are extracted and submitted as input to generate a list of the chemical perturbagens altering gene expression from the iLINCS portal, which is the third part of the report (22). The discordant perturbagens with a concordance score  $< -0.2$  and the concordant perturbagens with a concordance score  $> 0.2$  were identified. These perturbagens were grouped by their mechanism of action which was found using the L1000 fireworks and DrugBank databases (21). The iLINCS package was used to identify mechanisms of actions (MOAs) and gene targets for perturbagens that have a discordant signature to that

of the MC-LR vs. Vehicle comparison or concordant with MC-LR + Probiotic vs. MC-LR + Heat-Inactivated Probiotic and MC-LR + Probiotic vs. MC-LR. We looked at these specifically because signatures discordant with MC-LR vs. Vehicle may provide pathways that oppose MC toxin, while signatures concordant with the other two comparison groups may reveal potential therapeutic pathways to be targeted in future studies.

### 2.6. Figure Generation

The R package ggplot2 created the volcano plot using the differential gene expression data to show gene expression changes. *ComplexHeatmap* R package generated the enrichment score (ES) or combined score (CS) for pathways. PAVER (17), a text mining algorithm, clustered Gene Ontologies. The R Package ggplot2 created the correlation plots, which only included genes that are present in both comparisons.

### 2.7. Statistics

The *cor* function in R calculated the Pearson correlation coefficient between MC-LR + Probiotic vs. MC-LR and MC-LR + Probiotic vs. MC-LR + Heat-Inactivated Probiotic, which were moderately correlated with an *R-value* of .48 and p-value of  $< .001$ ; MC-LR Probiotic vs. MC-LR and MC-LR vs. Vehicle were more negatively correlated with an *R-value* of -0.63 and p-value  $< .001$ . The  $\log_2$  fold-change of common

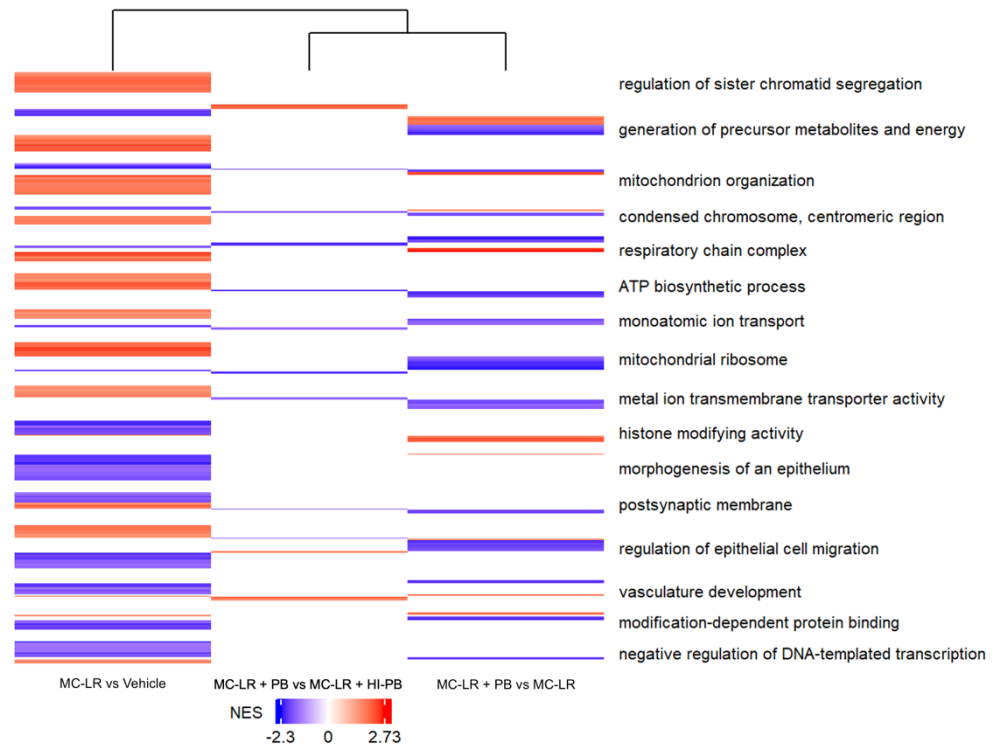


**Figure 4.** Heatmap comparing the differential gene expression of the three comparisons from GSEA clustered into groups shown in the right of the figure. To classify the pathways into hierarchical groups, PAVER analysis was performed. This further exemplifies the similarity between the groups comparing MC-LR with probiotic and MC-LR with and without heat-inactivated probiotic, suggesting that consistent with our hypothesis, the beneficial effects were due to the pre-treatment of live and active probiotic mixture, not attributable to any indirect effects caused by the presence of bacteria themselves. The Xs below each group indicate which pre-treatment they received. Abbreviations: PB, probiotic; HI-PB, heat-inactivated probiotic; MC-LR, Microcystin-leucine-arginine.

genes in each comparison were plotted as points on the correlation graph.

### 3. Results

Our results found that Probiotic attenuates the effect of MC-LR, and that Heat-Inactivated Probiotic does not. We also identified differences in gene expression between the comparisons in genes involved in metabolism, ribosomes, lipoproteins, and cytochrome P450. In addition, we found similarities between some groups' concordant and other groups' discordant MOAs and Gene Targets.

#### 3.1. DEG Heatmap

Combining the three comparisons, the differentially expressed genes (DEG) heatmap shows (1) MC-LR + Probiotic vs. MC-LR and (2) MC-LR + Probiotic vs. MC-LR + Heat-Inactivated Probiotic as having similar upregulated

and downregulated genes while MC-LR vs. Vehicle appears to be the inverse of the two. From this, it can be inferred that MC-LR and MC-LR + Heat-Inactivated Probiotic produce similar effects, while MC-LR + Probiotic and Vehicle also have similar effects. The heatmap is shown in Figure 2.

#### 3.2. Bivariate Correlation Plots

To confirm the correlation between MC-LR + Probiotic vs. MC-LR and MC-LR + Probiotic vs. MC-LR + Heat-Inactivated Probiotic, as seen in the DEG heatmap, we created a bivariate correlation plot shown in Figure 3A. There was a statistically significant ( $p < 0.001$ ) positive correlation between the two comparisons, suggesting that MC-LR and MC-LR + Heat-inactivated Probiotic have similar effects. This indicates that the heat-inactivated probiotic is ineffective at protecting the kidney from MC-LR, demonstrating that the activity of the

Symbol	Name	N	log <sub>2</sub> FC	p-value
<b>Upregulated</b>				
<b>Ndufa7</b>	NADH:ubiquinone oxidoreductase subunit A7	59	0.452	0.032
<b>Ndufs3</b>	NADH:ubiquinone oxidoreductase core subunit S3	53	0.497	0.005
<b>Ndufs6</b>	NADH:ubiquinone oxidoreductase core subunit S6	53	0.798	0.001
<b>Ndufs8</b>	NADH:ubiquinone oxidoreductase core subunit S8	53	0.592	<0.0001
<b>mt-Nd2</b>	mitochondrially encoded NADH dehydrogenase 2	53	0.63	<0.0001
<b>Ndufs1</b>	NADH:ubiquinone oxidoreductase core subunit S1	52	0.358	0.005
<b>Ndufs4</b>	NADH:ubiquinone oxidoreductase core subunit S4	52	0.746	0.001
<b>Birc5</b>	baculoviral IAP repeat-containing 5	50	1.509	0.004
<b>Ndufb6</b>	NADH:ubiquinone oxidoreductase subunit B6	50	0.82	<0.0001
<b>Ndufb7</b>	NADH:ubiquinone oxidoreductase subunit B7	50	0.541	0.002
<b>Downregulated</b>				
<b>Smarca4</b>	SWI/SNF related, matrix associated, actin dependent regulator of chromatin, subfamily a, member 4	54	-0.258	0.048
<b>Gata3</b>	GATA binding protein 3	47	-0.531	0.002
<b>Notch1</b>	notch 1	47	-0.586	0.004
<b>Tbx3</b>	T-box 3	45	-0.884	0.008
<b>Yap1</b>	yes-associated protein 1	44	-0.364	0.002
<b>Setd2</b>	SET domain containing 2	38	-0.428	0.01
<b>Nfatc1</b>	nuclear factor of activated T cells, cytoplasmic, calcineurin dependent 1	34	-0.5	0.005
<b>Crebbp</b>	CREB binding protein	33	-0.581	<0.0001
<b>Hdac7</b>	histone deacetylase 7	33	-0.449	0.007
<b>Jun</b>	jun proto-oncogene	33	-0.51	0.001

**Table 1.** Top 10 up and downregulated leading-edge genes for the MC-LR vs. Vehicle comparison. Abbreviations: MC-LR, Microcystin-leucine arginine; NADH, nicotinamide adenine dinucleotide + hydrogen; IAP, inhibitor of apoptosis; N, number of pathways gene is involved with; log<sub>2</sub>FC, log<sub>2</sub>Fold Change; DEGs, differentially expressed genes.

bacteria, not the presence of the bacteria alone, was responsible for the observed gene expression levels. Likewise, we created a bivariate correlation plot for MC-LR + Probiotic vs. MC-LR and MC-LR vs. Vehicle, which shows a statistically significant ( $p < 0.001$ ) negative correlation between the two comparisons (Fig. 3B). Since these two groups are statistically negatively correlated, this suggests that MC-LR and MC-LR + Probiotic have opposite effects. This implies that the probiotic effectively reverses the toxic effects of MC-LR.

### 3.3. GSEA PAVER Heatmap

A PAVER heatmap was generated to identify general reoccurring themes between upregulated and downregulated pathways (Fig. 4). The dendrograms at the top of the figure again indicate similarity between MC-LR + Probiotic vs. MC-LR and MC-LR + Probiotic vs. MC-LR + Heat-Inactivated

Symbol	Name	N	log <sub>2</sub> FC	p-value
<b>Upregulated</b>				
<b>Apoa4</b>	apolipoprotein A-IV	21	1.729	<0.0001
<b>Apoa1</b>	apolipoprotein A-I	20	1.132	<0.0001
<b>Apoa2</b>	apolipoprotein A-II	20	0.6	0.001
<b>Apoc3</b>	apolipoprotein C-III	19	0.487	0.029
<b>Apob</b>	apolipoprotein B	18	0.552	<0.0001
<b>Lcat</b>	lecithin cholesterol acyltransferase	16	0.74	0.02
<b>Apoa5</b>	apolipoprotein A-V	15	1.285	<0.0001
<b>Cyp7a1</b>	cytochrome P450, family 7, subfamily a, polypeptide 1	13	1.865	<0.0001
<b>Cyp2b13</b>	cytochrome P450, family 2, subfamily b, polypeptide 13	12	1.036	0.005
<b>Cyp2b9</b>	cytochrome P450, family 2, subfamily b, polypeptide 9	12	0.832	0.003
<b>Downregulated</b>				
<b>Ndufa7</b>	NADH:ubiquinone oxidoreductase subunit A7	40	-0.535	0.01
<b>Grin2d</b>	glutamate receptor, ionotropic, NMDA2D (epsilon 4)	34	-0.795	0.048
<b>Ndufs6</b>	NADH:ubiquinone oxidoreductase core subunit S6	34	-0.634	0.008
<b>Cacna2d1</b>	calcium channel, voltage-dependent, alpha2/delta subunit 1	33	-0.84	0.011
<b>mt-Nd2</b>	mitochondrially encoded NADH dehydrogenase 2	33	-0.342	0.045
<b>Ndufb6</b>	NADH:ubiquinone oxidoreductase subunit B6	32	-0.719	0.002
<b>Ndufs3</b>	NADH:ubiquinone oxidoreductase core subunit S3	32	-0.366	0.05
<b>Ndufs8</b>	NADH:ubiquinone oxidoreductase core subunit S8	32	-0.423	0.009
<b>Ndufs4</b>	NADH:ubiquinone oxidoreductase core subunit S4	31	-0.57	0.015
<b>Scn8a</b>	sodium channel, voltage-gated, type VIII, alpha	31	-1.75	0.003

**Table 2.** Top 10 up and downregulated leading-edge genes for the MC-LR + Probiotic vs. MC-LR comparison. Abbreviations: MC-LR, Microcystin-leucine arginine; PB, probiotic; NADH, nicotinamide adenine dinucleotide + hydrogen; N, number of pathways gene is involved with; log<sub>2</sub> FC, log<sub>2</sub> fold-change.

Probiotic. Notably, pathways relating to metabolism, cellular respiration, and nucleic acids appear frequently.

### 3.4. Volcano Plots

To quickly identify up and down regulated genes with respect to their log<sub>2</sub>-fold change and p-values, volcano plots were generated for each comparison. These are shown in Figure 5. The differential gene expression levels are on the x-axis, quantified by log<sub>2</sub> fold-change, and statistical

significance on the y-axis, measured by  $-\log_{10}$  (p-value). Notably, genes such as *Duxf3*, *Gm10800*, *Gm10801*, and *Gm26870*, are upregulated in MC-LR vs. Vehicle and downregulated in MC-LR + Probiotic vs. MC-LR.

### 3.5. MC-LR vs. Vehicle

To first characterize the effects of microcystin exposure on the kidney, we compared transcriptomes of mice exposed to MC-LR challenge vs. Vehicle control. In the EnrichR pathway

Symbol	Name	N	log <sub>2</sub> FC	p-value
<b>Upregulated</b>				
<b>Cyp4a10</b>	cytochrome P450, family 4, subfamily a, polypeptide 10	8	2.031	<0.0001
<b>Cyp4a12b</b>	cytochrome P450, family 4, subfamily a, polypeptide 12B	8	1.46	0.001
<b>Cyp4a14</b>	cytochrome P450, family 4, subfamily a, polypeptide 14	8	2.33	0.002
<b>Cyp4a31</b>	cytochrome P450, family 4, subfamily a, polypeptide 31	8	0.946	0.025
<b>Cyp4a32</b>	cytochrome P450, family 4, subfamily a, polypeptide 32	8	0.696	0.015
<b>Notch1</b>	notch 1	6	0.439	0.004
<b>Adgra2</b>	adhesion G protein-coupled receptor A2	5	0.307	0.026
<b>Efnb2</b>	ephrin B2	5	0.307	0.032
<b>Kdr</b>	kinase insert domain protein receptor	5	0.579	0.001
<b>Nr4a1</b>	nuclear receptor subfamily 4, group A, member 1	5	1.028	<0.0001
<b>Downregulated</b>				
<b>Ndufa1</b>	NADH:ubiquinone oxidoreductase subunit A1	12	-0.322	0.013
<b>Ndufb8</b>	NADH:ubiquinone oxidoreductase subunit B8	12	-0.261	0.021
<b>Ndufs8</b>	NADH:ubiquinone oxidoreductase core subunit S8	12	-0.255	0.021
<b>Ndufb11</b>	NADH:ubiquinone oxidoreductase subunit B11	12	-0.226	0.032
<b>Ndufa5</b>	NADH:ubiquinone oxidoreductase subunit A5	12	-0.233	0.043
<b>Ndufb10</b>	NADH:ubiquinone oxidoreductase subunit B10	12	-0.198	0.044
<b>Ndufa13</b>	NADH:ubiquinone oxidoreductase subunit A13	12	-0.232	0.047
<b>Cox5b</b>	cytochrome c oxidase subunit 5B	11	-0.234	0.048
<b>Atp1a3</b>	ATPase, Na <sup>+</sup> /K <sup>+</sup> transporting, alpha 3 polypeptide	10	-2.689	<0.0001
<b>Ndufa12</b>	NADH:ubiquinone oxidoreductase subunit A12	10	-0.262	0.03

**Table 3.** Top 10 up and downregulated leading-edge genes for the MC-LR + Probiotic vs. MC-LR + Heat-Inactivated Probiotic comparison. Abbreviations: MC-LR, Microcystin-leucine arginine; PB, probiotic; HI-PB, heat-inactivated probiotic; NADH, nicotinamide adenine dinucleotide + hydrogen; N, number of pathways gene is involved with; log<sub>2</sub>FC, log<sub>2</sub> fold-change.; DEGs differentially expressed genes

analysis, the top ten upregulated pathways are all related to cellular respiration and metabolism. See Supplementary Table 1 for the full results. For EnrichR pathways, a total of 114 significantly altered pathways were identified in MC-LR vs. Vehicle (adjusted p-value ≤ 0.05). In the top 90% of DEGs (N = 997) by log<sub>2</sub>FoldChange (>0.56 or -0.405<), there were 45 up-regulated pathways.

Similarly, we found all the top ten enriched GSEA pathways were also related to cellular respiration,

mitochondrial processes, or ribosomes. GSEA found a total of 418 significantly altered pathways in MC-LR vs. Vehicle (adjusted p-value ≤ 0.05). The detailed results of these analyses are shown in the Supplementary Table 2. Of which, 3 Pod Reports identified 230 up-regulated pathways containing 1,289 leading edge genes out of 6,068 pathways tested.

Some of the top leading-edge genes from GSEA pathways included *Ndufs1*, *Ndufs3*, *Ndufs4*, *Ndufs6*, *Ndufa7*, *Ndufs8*,

Themes	MC-LR vs. Vehicle		MC-LR + PB vs. MC-LR		MC-LR + PB vs. MC-LR + HI-PB	
	Up	Down	Up	Down	Up	Down
Electron transport chain	X			X		X
NADH dehydrogenase	X			X		X
Ribosomal Subunit	X			X		
Histone modification		X				
Chromatin organization		X				
Lipoprotein particle			X			
Steroid metabolic process			X			
Cytochrome P450			X		X	
Fatty Acid Metabolism					X	

**Table 4.** Summary table indicating main themes from different comparisons. The themes were picked from EnrichR, GSEA, and GSEA leading Edge gene tables from the three comparisons (see full tables in Supplemental Materials). These themes may warrant further discussion. Abbreviations: MC-LR, Microcystin-leucine arginine; PB, probiotic; HI-PB, heat-inactivated probiotic.

which all code for subunits of the mitochondrial membrane respiratory chain NADH dehydrogenase (complex 1). Other top leading-edge genes included *Plk1* and *Cenpe*, which code for proteins that regulate the cell cycle, and *Birc5*, which encodes for proteins that inhibit apoptosis. The top leading-edge genes are shown in Table 1.

Most of the ten downregulated pathways from EnrichR involved histones, or the acetylation and methylation of DNA, as shown in Supplementary Table 3. In the bottom 10% of DEGs (N = 944) by log<sub>2</sub>FoldChange (-0.405<), there were 69 down-regulated EnrichR pathways. However, the top ten of the 188 total downregulated GSEA pathways in this comparison were related to protein-DNA complexes, regulation of transcription, chromatin organization/remodeling, epithelial morphogenesis, and cardiac development as shown in Supplementary Table 4.

The GSEA analysis produced over 1,887 downregulated leading-edge genes, the top ten include *Smarca4*, *Gata3*, *Tbx3*, *Yap1*, *Med1*, *Pitx2*, which all play a role in regulating transcription. Table 1 shows the full analysis.

### 3.6. MC-LR vs. MC-LR Probiotic

To next investigate the ability of the probiotic mixture to attenuate the impact of MC-LR exposure on the kidneys, we compared the MC-LR exposed vs. MC-LR + Probiotic pre-treatment groups. While the majority of EnrichR up-regulated pathways were related to lipoproteins or cholesterol metabolism, others were related to skeletal morphogenesis and Eicosanoid transport (Supplementary Table 5). There was a total of 102 significantly altered pathways identified in pre-treatment groups compared to control groups with MC-LR Probiotic vs. MC-LR (adjusted p-value ≤ 0.05) in the Top

90% of DEGs (N = 889) by log<sub>2</sub> fold-change. (>0.352). There were 56 up-regulated pathways.

The GSEA enriched pathways included lipoproteins, lipids, steroids, triglycerides, and their related activities and metabolic processes. A total of 168 significantly altered pathways were identified (adjusted p-value ≤ 0.05). Of which, 46 were up-regulated pathways containing 262 leading edge genes. The tables presenting these pathways are included in Supplementary Table 6.

Several of the top ten leading edge genes found in these pathways included *Apoa4*, *Apoa1*, *Apoa2*, *Apoc3*, *Apob*, and *Apoa5*, which are related to lipoproteins, and two others were related to the cytochrome P450 pathway.

In contrast to the MC-LR vs. Vehicle comparison, where many genes such as *Duxf3* were upregulated, the same genes in the MC-LR vs. MC-LR + Probiotic analysis were downregulated. This demonstrates an inversion of upregulated and downregulated genes in the two datasets which is shown in Fig. 4.

Using the lowest 10% of DEGs (N = 809) by log<sub>2</sub>FoldChange (<-0.514), there were 46 down-regulated pathways identified by EnrichR. Many of these downregulated pathways were related to mitochondria, oxidoreduction, respiration, and NADH processes (Supplementary Table 7). In contrast, the most downregulated GSEA pathways were related to ribosomes, respirasomes, mitochondria, and cytoplasm (Supplementary Table 8). Interestingly, many of these pathways such as respiratory chain complex, respirasome, mitochondrial respirasome, and inner mitochondrial membrane protein complex were upregulated in the MC-LR vs. Vehicle comparison. Overall, 122 were down-regulated pathways containing 911 leading

edge genes out of 6039 pathways tested. Bottom leading-edge genes include Ndufa7, Ndufs6, Ndufb6, Ndufs3, Ndufs7,

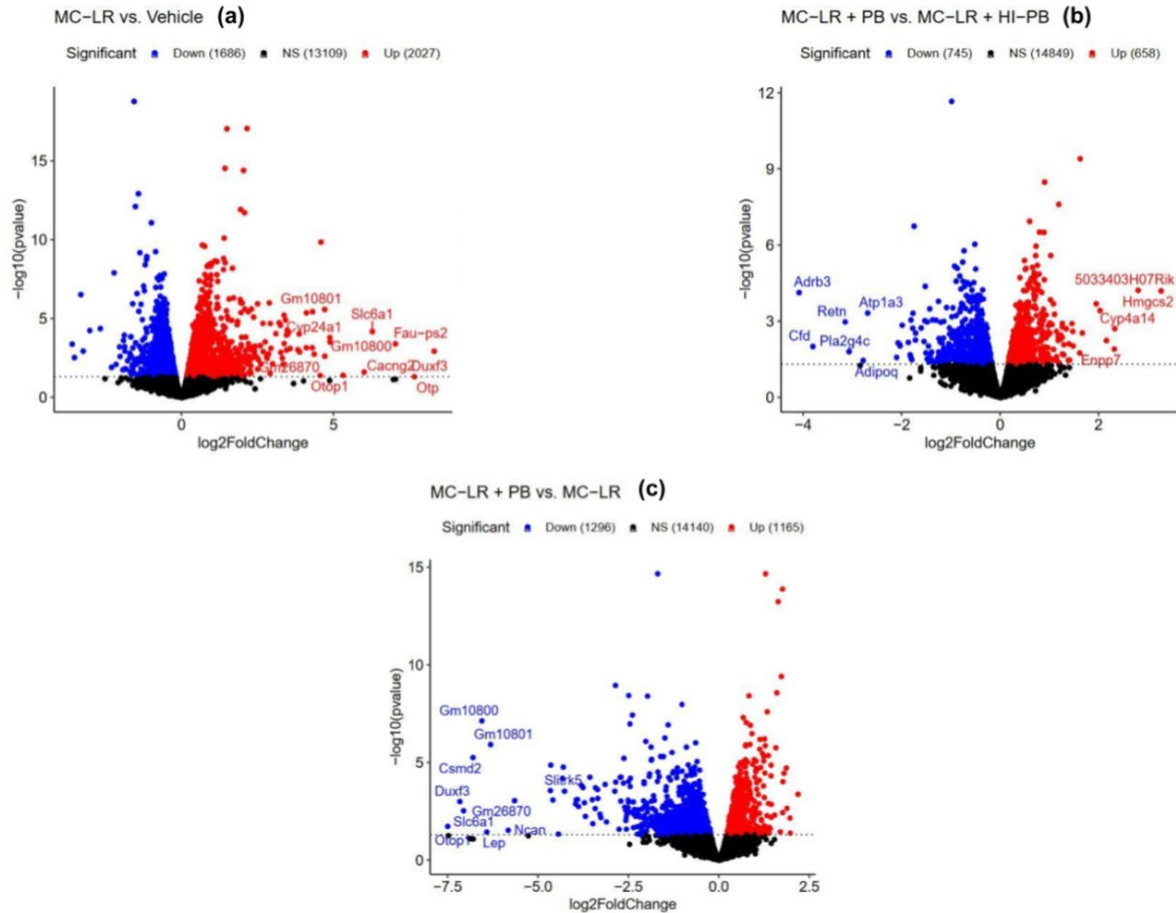


**Figure 5.** Volcano plot graphs demonstrating differential gene expression levels of (a) MC-LR vs. Vehicle (b) MC-LR + Probiotic vs. MC-LR + Heat-inactivated Probiotic (c) MC-LR + Probiotic vs. MC-LR. Gene expression levels in Figure 5(a) and Figure 5(c) are inverses of each other indicating strong differences between MC-LR and MC-LR + Probiotic as well as between Vehicle and MC-LR. The R package ggplot2 created the volcano plot using differential gene expression data collected by the experiment detailed above. Red represents genes with upregulated expression, blue represents down-regulated genes, and black means not significant, which means  $p > 0.05$ . The scale was maintained to allow visual comparison between the panels using the different axes.

which also all code for subunits of the mitochondrial membrane respiratory chain NADH dehydrogenase (complex 1). More details can be found in Table 2.

### 3.7. MC-LR + Probiotic vs. MC-LR + Heat-Inactivated Probiotic

To determine if differences between the control drinking water group and the probiotic drinking water group when exposed to MC-LR challenge were caused by the activity of the live bacteria and not merely indirect effects of the bacteria, the probiotic drinking water group and heat-inactivated probiotic drinking water group were compared after exposure to MC-LR. The top ten upregulated pathways from EnrichR included six that involved fatty acid metabolism, among others such as regulation of extracellular matrix assembly and regulation of glomerular filtration. Full details can be found in

Supplementary Table 9. There were a total of 106 significantly altered pathways (adjusted p-value  $\leq 0.05$ ) in the Top 90% of DEGs ( $N = 555$ ) using EnrichR by  $\log_2$  Fold-Change ( $>0.256$ ). Of these, 104 were upregulated EnrichR pathways.

For the top ten upregulated GSEA pathways, five involved catabolic processes and two increased eicosanoid synthesis and secretion. For MC-LR Probiotic vs. MC-LR heat-inactivated probiotic, a total of 39 significantly altered pathways were identified using GSEA (adjusted p-value  $\leq 0.05$ ). 16 were up-regulated pathways containing 186 leading edge genes. The top ten upregulated leading-edge genes included *Cyp4a10*, *Cyp4a12b*, *Cyp4a14*, *Cyp4a31*, and *Cyp4a32*, which encode cytochrome P450 proteins as seen in Table 3. These proteins catalyze reactions concerning drug metabolism and synthesis of lipids.

There were only two downregulated EnrichR pathways, long-term memory, and collagen-containing extracellular

OVERLAPPING MOAS	MC-LR VS. VEHICLE	MC-LR + PB VS. MC-LR	MC-LR + PB VS. MC-LR + HI-PB
VEGFR INHIBITOR	151	118	120
PDGFR TYROSINE KINASE RECEPTOR INHIBITOR	137	111	115
FLT3 INHIBITOR	118	110	109
HDAC INHIBITOR	130	101	105
CDK INHIBITOR	111	106	101
KIT INHIBITOR	109	92	97
DOPAMINE RECEPTOR ANTAGONIST	119	96	69

Table 5. Top overlapping MOAs that appeared in all comparison groups. These were picked from the detailed LINC analysis tables showing the top ten discordant MOAs for MC-LR vs. Vehicle and the top ten concordant MOAs for MC-LR + Probiotic vs. MC-LR and MC-LR + Probiotic vs. MC-LR + Heat-inactivated Probiotic, which are found in Supplementary Tables 13-15. Abbreviations: MC-LR, Microcystin-leucine arginine; PB, probiotic; HI-PB, heat-inactivated probiotic; MOA, mechanism of action.

matrix, both with relatively high p-values ( $>.01$ ) in the bottom 10% of DEGs (N =492) by  $\log_2$  fold-change. ( $<-0.321$ ) (Supplementary Table 11). Additionally, of the top ten downregulated GSEA pathways, nine involved cellular respiration (Supplementary Table 12). There were 23 down-regulated pathways containing 427 leading edge genes out of 5993 pathways tested. The top ten downregulated leading-edge genes included *Ndufa1*, *Ndufa2*, *Ndufa3*, *Ndufa5*, *Ndufa8*, *Ndufa9*, *Ndufa10*, *Ndufa11*, *Ndufa13*, and *Ndufb10* which code for complex I subunits that transfer electrons from NADH to ubiquinone. Refer to Table 3 for a complete list of the top downregulated leading-edge genes.

LINC analysis identifies the mechanisms of action (MOAs) and gene targets of perturbagens producing a discordant signature to that of the MC-LR vs. Vehicle comparison, and a concordant signature to that of MC-LR Probiotic vs. MC-LR and MC-LR Probiotic vs. MC-LR Heat-inactivated Probiotic. Further analysis found that several MOAs for the discordant MC-LR vs. Vehicle group, such as VEGFR inhibitor, PDGFR tyrosine kinase receptor inhibitor, and HDAC inhibitor also appeared in the top concordant MOAs for the other two comparison groups. Table 5 lists all overlapping MOAs and identifies them as potentially high yield pathways that could be targeted for therapeutic benefit. A full list of top MOAs for each individual comparison can be found in Supplementary Tables 13-15. Interestingly, several discordant MC-LR vs. Vehicle gene targets, such as EGFR, also appear in the top concordant gene targets MC-LR Probiotic vs. MC-LR and MC-LR Probiotic vs. MC-LR Heat-inactivated Probiotic. See Table 6 for all overlapping gene targets and refer to Supplementary Tables 16-18 for lists of the top gene targets in each comparison.

## 4. Discussion

As MC-LR is a potent toxin released during cyanoHABs, treatments for it have been a subject of investigation. We investigated if pre-treatment with MC-LR-degrading bacteria can reduce its effects in the kidney through differential gene expression data analysis. We found that probiotic pre-treatment reverses the transcriptional effect of MC-LR which makes it like Vehicle. We observed this visually through the shared heat map and statistically with the correlation plots [Fig 2, 3]. We found significant differences in gene expression both between and within the comparisons. This analysis revealed several key common themes in up and downregulated genes related to mitochondria, cellular respiration, ribosomes, lipoproteins, and Cytochrome P450.

### 4.1. Mitochondria and Cellular Respiration

Other studies have also looked at the effect of MCs on mitochondria, the organelle responsible cellular respiration. In particular, one study tested the effects of MC-RR and -LR on rabbit liver and hearts (23). They found damage to mitochondria in both organs and focused on how microcystin affects cellular respiration by inhibiting NADH dehydrogenase activity (complex 1) (23). NADH dehydrogenase is the first enzyme in the respiratory electron transport chain and catalyzes the electron transfer from NADH to ubiquinone while pumping a proton out of the matrix (24).

In our study, we found that the pathways and expression of genes related to metabolism was upregulated in the MC-LR vs. Vehicle comparison but downregulated in MC-LR + Probiotic vs. MC-LR and MC-LR + Probiotic vs. MC-LR + Heat-Inactivated Probiotic. There was increased expression in

SYMBOL	MC-LR VS. VEHICLE	MC-LR + PB VS. MC-LR	MC-LR + PB VS. MC-LR + HI-PB	NAME
<b>Number of Gene Targets</b>				
<b>EGFR</b>	42	29	25	epidermal growth factor receptor
<b>KDR</b>	39	26	32	kinase insert domain receptor
<b>MTOR</b>	32	29	23	mechanistic target of rapamycin kinase
<b>KIT</b>	26	19	23	KIT proto-oncogene, receptor tyrosine kinase

**Table 6.** Top overlapping perturbation gene targets found in all comparisons. These were picked from the detailed LINCS analysis tables showing the top ten discordant gene targets for MC-LR vs. Vehicle and the top ten concordant gene targets for MC-LR + Probiotic vs. MC-LR and MC-LR + Probiotic vs. MC-LR + Heat-inactivated Probiotic, which are found in Supplementary Tables 16-18.

the groups with mice exposed to MC-LR without any pre-treatment and mice exposed to MC-LR having received the heat-inactivated probiotic pre-treatment. The expression of genes and pathways related to the mitochondria was higher when these groups were in the numerator and lower when in the denominator of comparisons. This supports our hypothesis as it suggests some sort of compensation for its inhibition with increased expression and suggests the probiotic reduces this effect.

As mentioned previously, oxidative stress in cells is a major mechanism of MC-LR-exposed toxicity, which is caused by an increase in reactive oxygen species (ROS) and a decrease in antioxidant levels (11). Interestingly, ROS primarily originate from the mitochondrial transport chain during oxidative phosphorylation (11). Specifically, the main source of ROS formation, as demonstrated *in vitro* and *in vivo*, is up to 2% electron leakage from respiratory complex I and complex III before they are reduced to water at cytochrome c (25-27). This electron leakage mediates the reduction of oxygen to superoxide ( $O_2^{\cdot-}$ ), a ROS (25, 28, 29).

Our results are in line with this information because pathways pertaining to mitochondrial processes such as mitochondrial respirasome, respiratory chain complex, respirasome, and inner mitochondrial membrane protein complex were upregulated in the MC-LR vs. Vehicle comparison. This suggests that when mice are exposed to MC-LR without any probiotic pre-treatment, mitochondrial activity increases, allowing more electrons to leak. This generates more reactive oxygen species, increasing oxidative stress. In contrast, the same pathways relating to mitochondrial function and cellular respiration were downregulated in the MC-LR + PB vs. MC-LR comparison and the MC-LR + PB vs. MC-LR + HI-PB comparison groups. This suggests the mice that received a probiotic treatment experienced a decrease in mitochondrial activity, lowering the amount of ROS generated.

The effects of MC-LR exposure on mice lungs were studied with experimental groups given non-lethal doses of MC-LR for 20 days (30). Animals exposed to MC-LR had impaired

mitochondrial function with increased electron leakage and ROS formation in complex one of the electron transport chain (ETC) (30). Our results support this because mitochondrial pathways, many related to the ETC like mitochondrial respirasome, respiratory chain complex, and respirasome, as well as genes that code for complex I subunits are upregulated when comparing MC-LR vs. Vehicle (Table 1-3). These can lead to more electron leakage and ROS from MC-LR because mitochondria and specifically complex I can generate ROS (25-27). The comparisons with MC-LR probiotic had mitochondrial, and ETC complex I pathways downregulated, suggesting less ROS and effects from MC-LR (Table 1-3).

#### 4.2. Ribosome

Furthermore, studies have investigated the effect of microcystin on ribosome genes. One study tested the effects of MC-LR on seven ribosomal protein genes in carp organs using Q-PCR (31). It found an increase in expression in those ribosomal genes after exposure to MC-LR, which it suggested was a result of greater protein expression overall in response to MC-LR exposure (31). This is because ribosomes facilitate the translation of proteins, and the expression of those genes also decreased over time as the level of MC-LR in measured areas was reduced (31). Our study found increases in the differential expression of pathways related to ribosomes in MC-LR vs. Vehicle and a decrease in MC-LR Probiotic vs. MC-LR, which supports the other study as having exposure to just MC-LR resulted in higher expression compared to groups without MC-LR or with probiotic. Our results also suggest that the probiotic reduced the response to MC-LR because there may not be as much of MC-LR absorbed, leading to less expression of ribosome genes.

#### 4.3. Lipoproteins

Additionally, studies have investigated the effect of microcystin on lipid metabolism. A cross-sectional study evaluating the effects of microcystin on blood lipids and dyslipidemia found that the amount of microcystin exposure and the risk of dyslipidemia showed a dose-response

relationship. Microcystin exposure was also associated with increased triglyceride levels and decreased high-density lipoprotein cholesterol levels (32). This is supported by a study that examined the effects of MC-LR exposure on lipid metabolism in mice, which discovered that serum triglyceride and low-density lipoprotein cholesterol levels were increased while high-density lipoprotein cholesterol levels were decreased in mice exposed to MC-LR (33). In our analysis, high-density lipoprotein pathways were upregulated in the MC-LR Probiotic vs. MC-LR comparison, which shows that the effects of MC-LR were reversed. Furthermore, it was concluded that MC-LR exposure blocks fatty acid beta-oxidation while increasing enzymes for lipid synthesis (33). The former is consistent with our results because the MC-LR + Probiotic vs. MC-LR + Heat-Inactivated Probiotic comparison saw upregulated fatty acid beta-oxidation pathways, meaning that the probiotic reversed the signature of MC-LR. However, the latter is inconsistent with our results because the MC-LR + Probiotic vs. MC-LR + Heat-Inactivated Probiotic comparison showed upregulated eicosanoid synthesis and secretion. This may be because the increased lipid synthesis associated with MC-LR exposure may not refer to eicosanoids specifically.

#### 4.4. Cytochrome P450

Additionally, other studies have inquired on the effect of microcystin on cytochrome P450s. One study by Zhang et al. looked at the effect of MC-LR on the expression of certain cytochrome P450s in mouse liver using PCR (34). It found unchanged expression for CYP1A1 and increased expression for CYP3A11 at doses and measurement times most similar but still different to our study, with mixed results for the expression of those genes overall (34). In comparison, we found increased expression of CYP1A1 in MC-LR compared to vehicle and to MC-LR probiotic, as well as decreased expression of CYP3A11 in MC-LR compared to MC-LR probiotic (Supplementary Tables 19-21). These divergent results could be due to different target organs (liver vs. kidney), sequencing techniques (PCR vs. RNA sequencing), dosage (0-8 micrograms per kg vs. 500 micrograms of MC-LR), and time between measurements (1-7 days vs. 1 day).

#### 4.5. MOAs and Gene Targets

Finally, the LINCS analysis identified several MOAs that overlap between the discordant MC-LR vs. Vehicle group and the concordant MC-LR + Probiotic vs. MC-LR and MC-LR + Probiotic vs. MC-LR + Heat-Inactivated Probiotic groups. These overlapping MOAs may be high yield targets for future therapeutic intervention, including vascular endothelial growth factor receptor (VEGFR) inhibitors, PDGFR tyrosine kinase receptor inhibitor, and FLT3 inhibitor [Table 5]. VEGFR inhibitors were unanimously the top MOA for each comparison and would be of particular interest. Fortunately,

previous studies have looked at how MC-LR affects VEGFR. One study found that MC-LR facilitates the downregulation of mRNA expression of angiogenesis-related signaling molecules contributing to obesity, including VEGFR-2 (35). Our findings contradict these results since VEGFR inhibitor was identified as a discordant MOA to MC-LR vs. Vehicle, meaning that inhibiting VEGFR should reverse the effects of MC-LR. However, this difference in results could be due to varying experimental methods using different cell types. The researchers in the former study used human umbilical vein endothelial cells (HUVECs) to investigate the effects of MCs on the gene expression of signaling molecules, including VEGFR, while our study used kidney tissues from mice to identify the effects of MC-LR.

In addition to overlapping MOAs, the LINCS analysis also revealed several common gene targets for perturbagens discordant to MC-LR vs. Vehicle and concordant to MC-LR + Probiotic vs. Vehicle or Heat-Inactivated Probiotic. These include EGFR, KDR, MTOR, and KIT (Table 6). Past studies have identified epidermal growth factor receptor (EGFR) as a key gene in the malignant transformation induced by MC-LR, as well as a renal function indicator (RFI) (36). In a cross-sectional study conducted in Southwest China, researchers found that participants with abnormal RFIs had a much higher mean level of microcystin-LR estimated daily intake than those with normal (36). Particularly, those with lower levels of EGFR expression were associated with higher MC-LR (36). Our results are in line with theirs because EGFR was identified as a discordant gene target to MC-LR vs. Vehicle, suggesting that increased EGFR expression would behave similarly to the probiotic, reversing the effects of MC-LR on the kidneys.

## 5. Conclusion

We present the first analysis of the impact of microcystin on the mouse kidney in the presence and absence of a probiotic mixture. Our results have identified a number of key pathways using a variety of methods in agreement with existing literature, suggesting their involvement in microcystin toxicity. Furthermore, using a novel iLINCS approach, we identified pathways that could be targeted for future therapies for microcystin toxicity. Future study is warranted to validate these findings.

## References

- [1] Lad, A., J.D. Breidenbach, R.C. Su, J. Murray, R. Kuang, A. Mascarenhas, J. Najjar, S. Patel, P. Hegde, M. Youssef, J. Breuler, A.L. Kleinhenz, A.P. Ault, J.A. Westrick, N.N. Modyanov, D.J. Kennedy, and S.T. Haller, *As We Drink and Breathe: Adverse Health Effects of Microcystins and Other Harmful Algal Bloom Toxins in the Liver, Gut, Lungs and Beyond*. Life (Basel), 2022. 12(3).
- [2] Chorus, I., Introduction: Cyanotoxins — Research for Environmental Safety and Human Health, in *Cyanotoxins*:

- Occurrence, Causes, Consequences, I. Chorus, Editor. 2001, Springer Berlin Heidelberg: Berlin, Heidelberg. p. 1-4.
- [3] What is a harmful algal bloom? April 27, 2016 [cited; Available from: <https://www.noaa.gov/what-is-harmful-algal-bloom>.
- [4] Harke, M.J., M.M. Steffen, C.J. Gobler, T.G. Otten, S.W. Wilhelm, S.A. Wood, and H.W. Paerl, A review of the global ecology, genomics, and biogeography of the toxic cyanobacterium, *Microcystis* spp. *Harmful Algae*, 2016. 54: p. 4-20.
- [5] Arman, T. and J.D. Clarke, *Microcystin Toxicokinetics, Molecular Toxicology, and Pathophysiology in Preclinical Rodent Models and Humans*. *Toxins (Basel)*, 2021. 13(8).
- [6] Yoshizawa, S., R. Matsushima, M.F. Watanabe, K. Harada, A. Ichihara, W.W. Carmichael, and H. Fujiki, Inhibition of protein phosphatases by microcystins and nodularin associated with hepatotoxicity. *J Cancer Res Clin Oncol*, 1990. 116(6): p. 609-14.
- [7] Toivola, D.M., J.E. Eriksson, and D.L. Brautigam, Identification of protein phosphatase 2A as the primary target for microcystin-LR in rat liver homogenates. *FEBS Lett*, 1994. 344(2-3): p. 175-80.
- [8] Campos, A. and V. Vasconcelos, Molecular mechanisms of microcystin toxicity in animal cells. *Int J Mol Sci*, 2010. 11(1): p. 268-287.
- [9] Ito, E., A. Takai, F. Kondo, H. Masui, S. Imanishi, and K. Harada, Comparison of protein phosphatase inhibitory activity and apparent toxicity of microcystins and related compounds. *Toxicon*, 2002. 40(7): p. 1017-25.
- [10] Azevedo, S.M., W.W. Carmichael, E.M. Jochimsen, K.L. Rinehart, S. Lau, G.R. Shaw, and G.K. Eaglesham, Human intoxication by microcystins during renal dialysis treatment in Caruaru-Brazil. *Toxicology*, 2002. 181-182: p. 441-6.
- [11] Zhao, J., F. Tian, Q. Zhai, R. Yu, H. Zhang, Z. Gu, and W. Chen, Protective effects of a cocktail of lactic acid bacteria on microcystin-LR-induced hepatotoxicity and oxidative damage in BALB/c mice. *RSC Advances*, 2017. 7(33): p. 20480-20487.
- [12] Nybom, S.M., S.J. Salminen, and J.A. Meriluoto, Removal of microcystin-LR by strains of metabolically active probiotic bacteria. *FEMS Microbiol Lett*, 2007. 270(1): p. 27-33.
- [13] Thees, A., E. Atari, J. Birbeck, J.A. Westrick, and J.F. Huntley, Isolation and Characterization of Lake Erie Bacteria that Degrade the Cyanobacterial Microcystin Toxin MC-LR. *J Great Lakes Res*, 2019. 45(1): p. 138-149.
- [14] Breidenbach, J.D., B.W. French, T.T. Gordon, A.L. Kleinhenz, F.K. Khalaf, J.C. Willey, J.R. Hammersley, R. Mark Wooten, E.L. Crawford, N.N. Modyanov, D. Malhotra, J.G. Teeguarden, S.T. Haller, and D.J. Kennedy, Microcystin-LR aerosol induces inflammatory responses in healthy human primary airway epithelium. *Environ Int*, 2022. 169: p. 107531.
- [15] Lad, A., J. Hunyadi, J. Connolly, J.D. Breidenbach, F.K. Khalaf, P. Dube, S. Zhang, A.L. Kleinhenz, D. Baliu-Rodriguez, D. Isailovic, T.D. Hinds, Jr., C. Gatto-Weis, L.M. Stanoszek, T.M. Blomquist, D. Malhotra, S.T. Haller, and D.J. Kennedy, Antioxidant Therapy Significantly Attenuates Hepatotoxicity following Low Dose Exposure to Microcystin-LR in a Murine Model of Diet-Induced Non-Alcoholic Fatty Liver Disease. *Antioxidants (Basel)*, 2022. 11(8).
- [16] Su, R.C., J.D. Breidenbach, K. Alganem, F.K. Khalaf, B.W. French, P. Dube, D. Malhotra, R. McCullumsmith, J.B. Preslold, R.M. Wooten, D.J. Kennedy, and S.T. Haller, Microcystin-LR (MC-LR) Triggers Inflammatory Responses in Macrophages. *Int J Mol Sci*, 2021. 22(18).
- [17] Ryan, W., willgryan/PAVER: Pre-release to generate DOI. Zenodo.
- [18] Subramanian, A., P. Tamayo, V.K. Mootha, S. Mukherjee, B.L. Ebert, M.A. Gillette, A. Paulovich, S.L. Pomeroy, T.R. Golub, E.S. Lander, and J.P. Mesirov, Gene set enrichment analysis: a knowledge-based approach for interpreting genome-wide expression profiles. *Proc Natl Acad Sci U S A*, 2005. 102(43): p. 15545-50.
- [19] Gene Ontology, C., Gene Ontology Consortium: going forward. *Nucleic Acids Res*, 2015. 43(Database issue): p. D1049-56.
- [20] Kuleshov, M.V., M.R. Jones, A.D. Rouillard, N.F. Fernandez, Q. Duan, Z. Wang, S. Koplev, S.L. Jenkins, K.M. Jagodnik, A. Lachmann, M.G. McDermott, C.D. Monteiro, G.W. Gundersen, and A. Ma'ayan, Enrichr: a comprehensive gene set enrichment analysis web server 2016 update. *Nucleic Acids Res*, 2016. 44(W1): p. W90-7.
- [21] Xie, Z., E. Kropiwnicki, M.L. Wojciechowicz, K.M. Jagodnik, I. Shu, A. Bailey, D.J.B. Clarke, M. Jeon, J.E. Evangelista, V.K. M, A. Lachmann, A.A. Parigi, J.M. Sanchez, S.L. Jenkins, and A. Ma'ayan, Getting Started with LINCS Datasets and Tools. *Curr Protoc*, 2022. 2(7): p. e487.
- [22] Pilarczyk, M., M. Fazel-Najafabadi, M. Kouril, B. Shamsaei, J. Vasiliauskas, W. Niu, N. Mahi, L. Zhang, N.A. Clark, Y. Ren, S. White, R. Karim, H. Xu, J. Biesiada, M.F. Bennett, S.E. Davidson, J.F. Reichard, K. Roberts, V. Stathias, A. Koleti, D. Vidovic, D.J.B. Clarke, S.C. Schurer, A. Ma'ayan, J. Meller, and M. Medvedovic, Connecting omics signatures and revealing biological mechanisms with iLINCS. *Nat Commun*, 2022. 13(1): p. 4678.
- [23] Zhao, Y., P. Xie, R. Tang, X. Zhang, L. Li, and D. Li, In vivo studies on the toxic effects of microcystins on mitochondrial electron transport chain and ion regulation in liver and heart of rabbit. *Comp Biochem Physiol C Toxicol Pharmacol*, 2008. 148(3): p. 204-10.
- [24] Cermakova, P., A. Madarova, P. Barath, J. Bellova, V. Yurchenko, and A. Horvath, Differences in mitochondrial NADH dehydrogenase activities in trypanosomatids. *Parasitology*, 2021. 148(10): p. 1161-1170.
- [25] Ashrafi, G. and T.L. Schwarz, The pathways of mitophagy for quality control and clearance of mitochondria. *Cell Death Differ*, 2013. 20(1): p. 31-42.
- [26] Scialo, F., A. Sriram, D. Fernandez-Ayala, N. Gubina, M. Lohmus, G. Nelson, A. Logan, H.M. Cooper, P. Navas, J.A. Enriquez, M.P. Murphy, and A. Sanz, Mitochondrial ROS Produced via Reverse Electron Transport Extend Animal Lifespan. *Cell Metab*, 2016. 23(4): p. 725-34.
- [27] Chouchani, E.T., V.R. Pell, E. Gaude, D. Aksentijevic, S.Y. Sundier, E.L. Robb, A. Logan, S.M. Nadtochiy, E.N.J. Ord, A.C. Smith, F. Eyassu, R. Shirley, C.H. Hu, A.J. Dare, A.M. James, S. Rogatti, R.C. Hartley, S. Eaton, A.S.H. Costa, P.S. Brookes, S.M. Davidson, M.R. Duchon, K. Saeb-Parsy, M.J.

- Shattock, A.J. Robinson, L.M. Work, C. Frezza, T. Krieg, and M.P. Murphy, Ischaemic accumulation of succinate controls reperfusion injury through mitochondrial ROS. *Nature*, 2014. 515(7527): p. 431-435.
- [28] Goncalves, R.L., C.L. Quinlan, I.V. Perevoshchikova, M. Hey-Mogensen, and M.D. Brand, Sites of superoxide and hydrogen peroxide production by muscle mitochondria assessed ex vivo under conditions mimicking rest and exercise. *J Biol Chem*, 2015. 290(1): p. 209-27.
- [29] Kowalczyk, P., D. Sulejczak, P. Kleczkowska, I. Bukowska-Osko, M. Kucia, M. Popiel, E. Wietrak, K. Kramkowski, K. Wrzosek, and K. Kaczynska, Mitochondrial Oxidative Stress- A Causative Factor and Therapeutic Target in Many Diseases. *Int J Mol Sci*, 2021. 22(24).
- [30] Mesquita, F.M., D.F. de Oliveira, D.A.F. Caldeira, J.P.C. de Albuquerque, L. Matta, C.C. Faria, I.I.A. Souza, C.M. Takiya, R.S. Fortunato, J.H.M. Nascimento, S.M.F. de Oliveira Azevedo, W.A. Zin, and L. Maciel, Subacute and sublethal ingestion of microcystin-LR impairs lung mitochondrial function by an oligomycin-like effect. *Environ Toxicol Pharmacol*, 2022. 93: p. 103887.
- [31] Cai, Y., C. Zhang, L. Hao, J. Chen, P. Xie, and Z. Chen, Systematic identification of seven ribosomal protein genes in bighead carp and their expression in response to microcystin-LR. *J Toxicol Sci*, 2016. 41(2): p. 293-302.
- [32] Feng, S., M. Cao, P. Tang, S. Deng, L. Chen, Y. Tang, L. Zhu, X. Chen, Z. Huang, M. Shen, and F. Yang, Microcystins Exposure Associated with Blood Lipid Profiles and Dyslipidemia: A Cross-Sectional Study in Hunan Province, China. *Toxins (Basel)*, 2023. 15(4).
- [33] Chu, H., C. Du, Y. Yang, X. Feng, L. Zhu, J. Chen, and F. Yang, MC-LR Aggravates Liver Lipid Metabolism Disorders in Obese Mice Fed a High-Fat Diet via PI3K/AKT/mTOR/SREBP1 Signaling Pathway. *Toxins (Basel)*, 2022. 14(12).
- [34] Zhang, B., Y. Liu, and X. Li, Alteration in the expression of cytochrome P450s (CYP1A1, CYP2E1, and CYP3A11) in the liver of mouse induced by microcystin-LR. *Toxins (Basel)*, 2015. 7(4): p. 1102-15.
- [35] Khan, M.I., J.H. Shin, and J.D. Kim, Crude microcystins extracted from *Microcystis aeruginosa* exert anti-obesity effects by downregulating angiogenesis and adipogenesis related signaling molecules in HUVEC and 3 T3-L1 cells. *BMC Complement Altern Med*, 2019. 19(1): p. 100.
- [36] Lin, H., W. Liu, H. Zeng, C. Pu, R. Zhang, Z. Qiu, J.A. Chen, L. Wang, Y. Tan, C. Zheng, X. Yang, Y. Tian, Y. Huang, J. Luo, Y. Luo, X. Feng, G. Xiao, L. Feng, H. Li, F. Wang, C. Yuan, J. Wang, Z. Zhou, T. Wei, Y. Zuo, L. Wu, L. He, Y. Guo, and W. Shu, Determination of Environmental Exposure to Microcystin and Aflatoxin as a Risk for Renal Function Based on 5493 Rural People in Southwest China. *Environ Sci Technol*, 2016. 50(10): p. 5346-56.

## Funding Acknowledgements

This work was supported by a Harmful Algal Bloom Research Initiative grant from the Ohio Department of Higher Education (STH, JFH, AL, DJK), the David and Helen Boone Foundation Research Fund (STH, DJK), the University of Toledo Women and the Philanthropy Genetic Analysis Instrumentation Center (STH, DJK) and NIH NIGMS T32-G-RISE grant number 1T32GM144873-01 (WR).